



Preparation of mesoporous activated carbon from defective coffee beans for adsorption of fresh whey proteins

Giovanni Aleixo Batista¹, Maria Letícia Martins Silva¹, Willian de Paula Gomes¹, Isabelle Cristina Oliveira Neves¹, Paula Chequer Gouveia Mól², Jaime Vilela de Resende¹, Lizzy Ayra Alcântara Veríssimo^{1*} and Jenaina Ribeiro Soares³

¹Departamento de Ciências, Universidade Federal de Lavras, Av. Doutor Sylvio Menicucci, 1001, 37200-000, Lavras, Minas Gerais, Brazil. ²Departamento de Engenharia e Tecnologia de Alimentos, Universidade de São Paulo, São José do Rio Preto, São Paulo, Brazil. ³Departamento de Física, Universidade Federal de Lavras, Lavras, Minas Gerais, Brazil. *Author for correspondence. E-mail: lizzy.alcantara@ufla.br

ABSTRACT. Whey protein has high biological value and functional properties. Therefore, it is necessary to develop methods to recover this valuable protein and minimize the environmental impacts. Adsorptive processes using alternative adsorbents from agroindustrial waste increase the number of alternatives for adequate final disposal of the waste and add value. The aim of this study was to develop a mesoporous activated carbon (AC) from defective coffee beans (DCB) for the adsorption of fresh whey protein. The morphological structure of the adsorbent produced was characterized, and both Raman spectroscopy, FTIR and thermal analyses were performed; and the effect of pH on the adsorption capacity (q , mg g⁻¹) was evaluated. The characterization showed that: the AC exhibited a porous size between 33 and 43 Å, corresponding to mesoporous materials; the crystallite size (L_a) of AC was estimated at 9.31 ± 0.14 nm; the highest adsorption capacity value (239.1781 mg g⁻¹) was achieved at pH 2.5 and 25°C; and the point of zero charge of the adsorbent was at pH 2.0. The pseudo first-order model fit best to the experimental results ($R^2 > 0.99$) of whey protein adsorption onto activated carbon, and the Langmuir model was the most appropriate to represent the experimental data, with a maximum adsorption capacity of 378.4380 mg g⁻¹, demonstrating the potential of AC obtained from DCB to adsorb fresh whey protein.

Keywords: agroindustrial waste; adsorbent; isotherms; Raman spectroscopy; whey proteins.

Received on December 18, 2018
Accepted on July 17, 2019

Introduction

The activated carbon (AC) global market has presented an increasing growth, especially in the food (Pereira et al., 2014), pharmaceutical, medical industries (Santana et al., 2017) and energy storage devices (Arvind & Hegde, 2015), although its major use is still in water treatment and air purification (Roy, Das, & Sengupta, 2017; Santana et al., 2017).

Activated carbon presents a high specific surface area that is related to the target molecule to be adsorbed. Its great chemical and mechanical stability, in addition to the variety of possible functional groups existent on the carbon surface, enables it to be widely utilized instead of the classic adsorbents such as silica gel, activated alumina and molecular sieves (Pereira et al., 2014; Yang & Qiu, 2011).

Meso- and macro-porous activated carbon structures can be obtained by chemical activation, physical activation or a combination of both methods (Yang & Qiu, 2011). In chemical activation, the solid matrix is treated with a chemical compound that remains impregnated in the precursor material (PM), subsequently subjected to carbonization (Liou, 2010; Pereira et al., 2014). The presence of large pores makes the adsorbent suitable for adsorption of larger biomolecules (Andrade et al., 2018; Liou, 2010; Pereira et al., 2014; Yang & Qiu, 2011).

AC may be produced from a variety of carbonaceous materials. The use of agroindustrial waste has recently received attention due to the large amounts of raw material generated and its low cost, aggregating value to an industrial residue (Pereira et al., 2014; Yang & Qiu, 2011). Among these alternative materials, black, green and sour defective coffee beans (DCB) may be a potential source of an organic precursor for the

production of carbons, since these defective grains represents about 20% of total coffee production (Ramos, Guerreiro, Resende, & Gonçalves, 2009).

In addition to being a promising alternative source for the production of low-cost adsorbents, agroindustrial residues may also be used to recover biomolecules, such as proteins, from crude extracts. Whey has long been considered a waste byproduct from cheese production, representing about 90% milk volume, making its correct treatment environmentally important (Abd El-Salam & El-Shibiny, 2017; Ganju & Gogate, 2017; Prazeres, Carvalho, & Rivas, 2012). The advent of recovery technologies of whey constituents has increased its utilization (Abd El-Salam & El-Shibiny, 2017; Ganju & Gogate, 2017; Prazeres et al., 2012).

Several techniques have been applied for the recovery of whey protein, such as precipitation (Bogahawaththa, Chandrapala, & Vasiljevic, 2017; Eugenia Lucena, Alvarez, Menéndez, Riera, & Alvarez, 2007), membrane filtration (Baldasso, Barros, & Tessaro, 2011; Corbatón-Báguena, Álvarez-Blanco, & Vincent-Vela, 2018; Damar Huner & Gulec, 2017), adsorption (Andrade et al., 2018; Fontan, Minim, Bonomo, da Silva, & Minim, 2013; Sarvi et al., 2014) and others. Adsorption is highlighted as a strategy for whey protein recovery, and the use of activated carbon produced from agricultural residues appears to be a promising alternative to reduce the cost of the adsorption process (Bhatnagar, Sillanpää, & Witek-Krowiak, 2015).

Therefore, the aim of this study was to produce activated carbon from defective coffee beans as precursor material (PM) for adsorption of fresh whey protein. The present study conducted a broad characterization of the adsorbent synthesized from agroindustrial waste (structural, morphological, physical-chemical and thermal). Then, the effect of pH on the adsorptive capacity of whey protein by activated carbon was assessed. In addition, the mechanisms of whey protein adsorption kinetics were determined, as well as the adsorption isotherms. As a result, the application of AC in real samples, as the fresh whey without any previous treatments, and the obtaining of relevant results of adsorptive capacity is one of the greatest highlights of the study.

Material and methods

Preparation of fresh whey

Fresh whey was obtained from the production of Minas frescal cheese and was provided by the Laboratory of Milk and Dairy Products of the Federal University of Lavras, State of Minas Gerais, Brazil. Whey was composed of $0.787 \pm 0.078\%$ ash, $96.033 \pm 0.409\%$ moisture, $1.017 \pm 0.102\%$ protein, $0.700 \pm 0.000\%$ fat, $1.210 \pm 0.131 \text{ g L}^{-1}$ lactose and $0.100 \pm 0.000\%$ lactic acid. Whey was initially subjected to slow pasteurization at 63°C for 30 min. and diluted with sodium phosphate buffer 20 mmol L^{-1} (1:4, v/v) at different pH (2.5, 4.5, and 7.5). These values were chosen because they comprise the range of pH values for different types of whey (Ganju & Gogate, 2017). The protein solution was used in the adsorption assays and presented an average of 0.662 mg mL^{-1} of total protein, which was determined spectrophotometrically by the Bradford method at 595 nm (Bradford, 1976).

Preparation of activated carbon

Defective coffee beans (DCB) were used as carbon precursor material in the synthesis of activated carbon. DCB were kindly provided by the Coffee Excellence Pole of the Federal University of Lavras, State of Minas Gerais, Brazil. The precursor material was characterized in terms of moisture, ash, total nitrogen, glucose fraction, ether fraction and crude fiber contents according to the standards of the International Association of Official Analytical Chemists (AOAC) (AOAC, 2012).

Activated carbons were produced according to a methodology adapted from Pereira et al. (2014). First, DCB were impregnated with phosphoric acid (85% wt.) at a 3:1 mass ratio (activating agent: precursor material) and dried at 85°C for 24h. The material was then carbonized in a muffle furnace under ambient pressure at 500°C for 30 min. Then, carbon was washed with 5.0 mol L^{-1} HCl. Finally, activated carbon was rinsed with distilled water several times until the filtrate reached pH 7.0. It was then dried at 105°C for 24h, and ground and sieved through an 18-mesh sieve. The activated carbon yield was calculated by Equation 1.

$$Yield(\%) = \left(\frac{W_f}{W_0} \right) \times 100 \quad (1)$$

where: W_f and W_0 (g) are the weights of activated carbon and dried precursor material.

Characterization of prepared activated carbon

The morphology of the activated carbon was evaluated by scanning electron microscopy (SEM). Samples were dried at 105°C for 24h and manually fixed on stubs. Subsequently, they were coated with a gold layer and examined using a scanning electron microscope (LEO EVO 40 XVP, Zeiss, Cambridge, UK).

The functional groups on the AC surface were analyzed using Fourier transform infrared spectroscopy (FTIR). Direct readings were performed by attenuated total reflectance (ATR) in the infrared region of 4,000 to 500 cm^{-1} .

The point of zero charge (pHpzc) was determined by the method known as “experiment of 11 points” (Vieira et al., 2010).

A thermogravimetric analysis (TGA) was performed using a thermomechanical analyzer (Shimadzu-TMA50, Japan). Samples (6.2 mg) were heated at 10°C min^{-1} under an air stream from 25°C to 750°C.

The AC was evaluated in relation of the contents of carbon (C), hydrogen (H), nitrogen (N) and sulfur (S) using a universal analyzer (Vario Micro Cube, Elementar). The oxygen content was determined according to mass balance, and the ash content was determined according to the AOAC methodology (AOAC, 2012).

Raman spectra were acquired by using a Horiba LabRAM HR Evolution spectrometer equipped with a Synapse Charge Coupled Device (CCD) detector, an Olympus BX41 microscope, and a 50 × objective lens in the backscattering configuration. Spectra were collected on three different points for each sample. The excitation laser used was the 532 nm green line, with power maintained below 200 microW, and three accumulations of ten seconds for each spectrum were performed, from 500 to 2,000 cm^{-1} .

The N_2 adsorption and desorption isotherms were obtained by a Micromeritics device (model ASAP 2420), using approximately 0.20 g material. Samples were previously treated at 120°C, followed by evacuation at 30°C for 30 min., and heated again at a rate of 10°C min^{-1} until 200°C, remaining at this temperature for 300 min. Subsequently, isotherms were obtained at 77 K.

The specific surface area was determined by the BET equation. Pore size distribution was obtained from the BJH method, while the volume of micropores was determined by t-plot analysis.

Adsorption assays

Whey protein adsorption was investigated as a function of pH (2.5, 4.5, and 7.5) in a completely randomized design with three repetitions. The adsorption assays were conducted in a batch process in stirred tanks using 0.01 g AC added to 10 mL of the buffer containing fresh whey protein (about 0.662 mg mL^{-1} of protein). Samples were maintained under light stirring at 25°C for 24h (Pereira et al., 2014). The tubes were then centrifuged (4,680 $\times g$ for 30 min.), and the supernatant was collected for quantification of total protein by the Bradford method (Bradford, 1976). The blank of the readings corresponded to the phosphate buffer 20 mmol L^{-1} at different pH values (2.5, 4.5, and 7.5), without the addition of whey. The calibration curve was constructed with bovine serum albumin ranging from 0.1 mg mL^{-1} to 1.0 mg mL^{-1} . All assays were performed in triplicate.

The carbon adsorptive capacity was determined from the difference between the initial and final protein content, using Equation 2.

$$q = \frac{(c_0 - c) \cdot V}{m} \quad (2)$$

where: q is the amount of protein adsorbed at equilibrium (mg g^{-1}); c_0 and c are the initial and final concentrations of the protein in solution, respectively (mg mL^{-1}); V is the solution volume (mL); and m is the mass of the adsorbent (g).

Kinetics of the whey proteins adsorption

Adsorption kinetics assays were performed at 25°C during 24h (Pereira et al., 2014). Samples of 0.01 g AC were added to centrifuge tubes with 10 mL sodium phosphate solution (20 mmol L^{-1} , pH 2.5) containing the

fresh whey protein (0.353 mg mL⁻¹). Aliquots of the supernatant were collected at 1h intervals, and the protein concentration was determined by the Bradford (1976) method. All assays were performed in triplicate.

The adsorption kinetic models are usually described by the pseudo first-order (Equation (3)), pseudo second-order (Equation (4)) and intraparticle diffusion models for most of the adsorbent-adsorbate systems (Ho & McKay, 1998). The pseudo first-order model is given by Equation 3:

$$\ln(q_e - q_t) = \ln q_e - k_1 t \quad (3)$$

where: q_e and q_t are the adsorption capacities (mg g⁻¹) at equilibrium and at time t (min), respectively, and k_1 is the rate constant of pseudo first-order adsorption (min.⁻¹).

The pseudo second-order is given by Equation 4:

$$q_t = \frac{t}{\frac{1}{k_2 q_e^2} + \frac{t}{q_e}} \quad (4)$$

where: k_2 is the rate constant of second-order adsorption (g mg⁻¹ min.⁻¹), and q_e and q_t are the adsorption capacities (mg g⁻¹) at equilibrium and at time t (min.), respectively. The constant k_2 is used to calculate the rate of initial adsorption h (mg g⁻¹ min.⁻¹) (Equation 5), at t_0 :

$$h = k_2 q_e^2 \quad (5)$$

The intraparticle diffusion model is given by Equation 6 (Ho & McKay, 1998):

$$q = k_{dif} t^{1/2} + k \quad (6)$$

where: q is the adsorption capacity (mg g⁻¹) at time t (h), k_{dif} is the intraparticle diffusion rate constant (mg g⁻¹ h^{-1/2}), and k is a constant related to the diffusion resistance (mg g⁻¹).

The kinetics parameters of the adsorption process were obtained by non-linear regression using SAS® University Edition and the models were evaluated according to the coefficient of determination (R²), and the root mean square error (RMSE).

Adsorption isotherms

Different initial concentrations of protein in the solution were obtained for the fresh whey (1.3871 mg mL⁻¹ of total protein) diluted with sodium phosphate buffer (20 mmol L⁻¹, pH 2.5) at the proportions of 1:1, 1:2, 1:3, 1:4, 1:5, 1:6, 1:7, 1:10, 1:12, 1:14, and 1:20, which resulted in initial protein concentrations ranging from 0.1036 to 1.3871 mg mL⁻¹.

Adsorption isotherms of fresh whey protein on AC were investigated in a batch process at pH 2.5 and 25°C. A 0.01 g mass of dried activated carbon was incubated with 10 mL of protein solution obtained by the whey dilutions and was maintained under gentle stirring for 24h. The total protein content in the supernatant and initial concentration were determined according to the method of Bradford (1976). All experiments were conducted in triplicate. The amount of adsorbed proteins was then determined by mass balance (Equation 2).

The Langmuir and Freundlich isotherms (Equation 7 and 8) were fitted to the equilibrium data. Model parameters were estimated by a non-linear regression using SAS® University Edition

$$q = \frac{q_{max} C}{K_d + C} \quad (7)$$

where: q_{max} is the maximum adsorption capacity (mg g⁻¹), c is the protein concentration in the solution after reaching equilibrium (mg mL⁻¹), and K_d is the dissociation constant (mg mL⁻¹).

$$q = K_f C^n \quad (8)$$

where: K_f is the Freundlich isotherm constant (mL mg⁻¹), and n is a constant for this isotherm (dimensionless).

Results and discussion

Characterization of the activated carbon

The composition of the precursor material consisted of 9.59% moisture, 3.51% ash, 13.10% total nitrogen, 58.38% glucose fraction, 5.90% ethereal extract, and 9.52% crude fiber. The yield of AC from DCB

was 29.68%. Yield values found in the present work are in accordance with those found by Hirata et al. (2002) for AC produced from coffee grounds and Pereira et al. (2014) for AC produced from the shell of *Theobroma cacao*.

The precursor sample showed low ash content (3.51%), which is beneficial in the carbon activation process since minerals preferentially adsorb water due to its hydrophilic content (Table 1). After chemical activation and carbonization of the precursor, the AC obtained from DCB presented a low ash content (3.78%), which may positively affect the adsorption capacity (Ramos et al., 2009).

Table 1. Elemental analysis (CHNO) of the precursor material (PM) and activated carbon (AC) from defective coffee beans (DCB).

Sample	C (%)	H (%)	N (%)	S (%)	O (%)	C/H
PM	44.48 ± 0.00	6.63 ± 0.03	2.87 ± 0.10	0.09 ± 0.02	45.93 ± 0.15	6.71 ± 0.03
AC from DCB	81.11 ± 0.32	3.47 ± 0.10	1.76 ± 0.06	0.01 ± 0.00	13.66 ± 0.34	23.39 ± 0.71

Fourier transform infrared spectroscopy (FTIR)

FTIR spectra of the precursor material samples (defective coffee beans) and the AC produced from DCB are illustrated in Figure 1A and B, respectively. According to Figure 1A, the vibration frequencies from 2,922 to 2,854 cm^{-1} are characteristic of symmetrical and asymmetric vibrations of methyl and methylene groups (Ramos et al., 2009). The absorption at 1,746 cm^{-1} is typical of carbonyl (C = O) vibrational stretching of potentially carboxylic acids, aldehydes or δ -lactones. Absorption located at 1,645 cm^{-1} is related to C = O stretching vibration of amides (Ramos et al., 2009). The absorption at 1,032 cm^{-1} might be attributed to the C - O stretching in lignin, cellulose or hemicellulose, or C - O - C in cellulose and hemicellulose (Vieira et al., 2010).

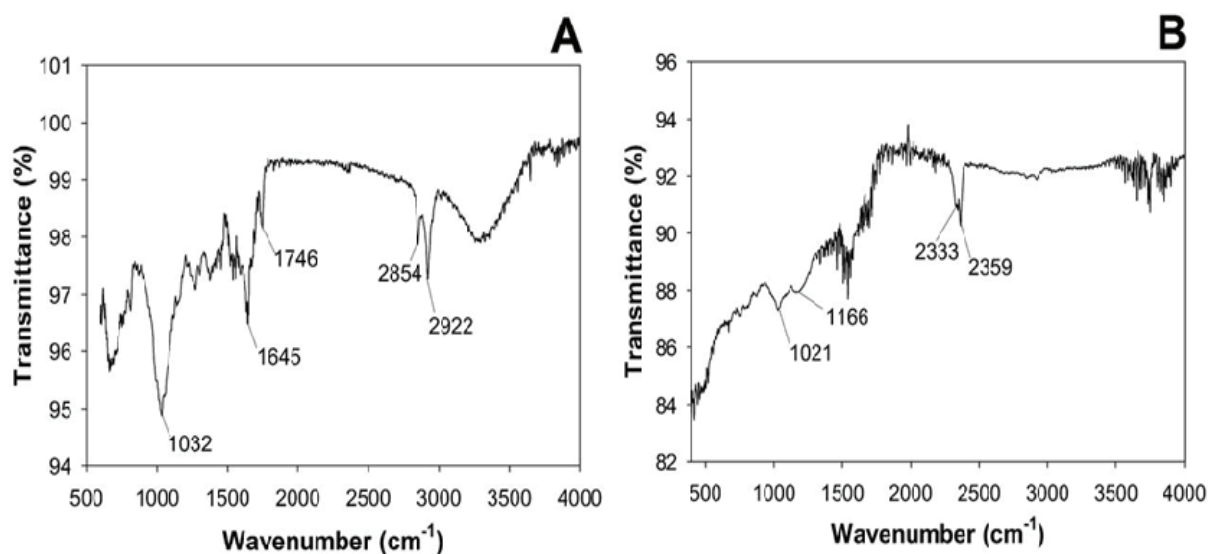


Figure 1. FTIR spectra of the precursor (A) and activated carbon produced from defective coffee beans (B).

After activation and carbonization of the precursor material, a decrease of the bands referring to functional groups present in the DCB can be observed (Figure 1B). Weak absorptions at 1,021 and 1,166 cm^{-1} present in the AC are assigned to C - O stretching of ethers (Brito et al., 2017). Weak absorptions at 2,333 cm^{-1} are attributed to C - H aliphatic stretching (Ramos et al., 2009) and adsorption at 2,359 cm^{-1} is characteristic of methyl groups (Pereira et al., 2014).

Scanning electron microscopy (SEM)

Activated carbon produced from the DCB presented an irregular granular structure and a rough surface with few developed pores (Figure 2). Ramos et al. (2009) obtained a different structure for DCB activated carbon. Such divergences may be related to the use of phosphoric acid as the activating agent and to the carbonization protocol, which was free of nitrogen flow and lasted only 30 min.

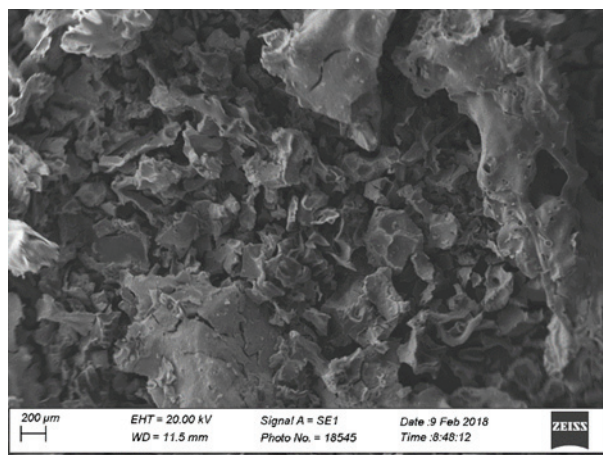


Figure 2. SEM micrographs of the activated carbon prepared from defective coffee beans. 50x magnification.

Thermogravimetry analysis (TGA)

The thermogram of AC obtained from defective coffee beans is shown in Figure 3. Three significant thermal events stand out. The first step (up to 170°C) may be attributed to the loss of water and volatile compounds originally present in the sample (Fritzen-Freire et al., 2012; Ramos et al., 2009). In the second stage, the activated carbon undergoes severe thermal decomposition from 450 to 700°C, with a pronounced mass loss (79.03%) possibly due to depolymerization, pyrolysis, and degradation of phenolic compounds, polysaccharides and other components (Hosseini, Zandi, Rezaei, & Farahmandghavi, 2013; Ramos et al., 2009). In the third stage, the residual mass of the samples is small enough to indicate nearly complete thermal degradation (approximately 91.12 to 93.54%).

The activated carbon has excellent thermal stability throughout this temperature range, and a small mass loss is observed between 25 and 170°C (± 0.4 mg), which corresponds to a loss of approximately 6.45% of its initial mass.

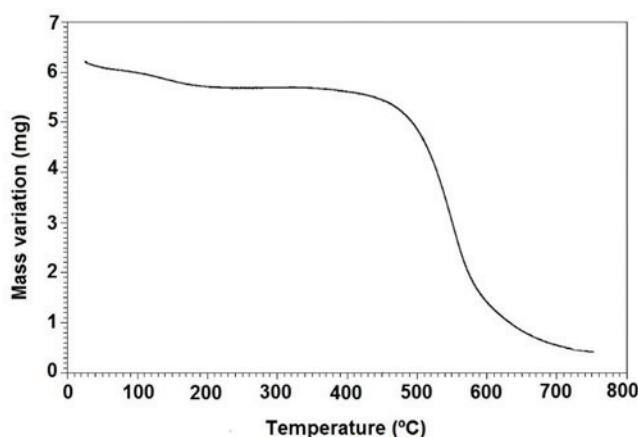


Figure 3. TGA curves of the activated carbon obtained from defective coffee beans.

Surface area and porosity analysis (BET)

As can be seen in Figure 4, the N_2 adsorption/desorption isotherm of the prepared activated carbon can be classified as type IV, which is characteristic of mesoporous materials (IUPAC - International Union of Pure and Applied Chemistry, 1985). In the isotherm curve (Figure 4), the wide hysteresis loop at high relative pressures may be associated with micro- and mesoporous structures of the produced activated carbons (Gonçalves et al., 2013; Jain & Tripathi, 2014; Lim, Srinivasakannan, & Balasubramanian, 2010). The pore size distribution can be visualized in Figure 4B, and it shows that the activated carbon exhibited an important contribution between 33 and 43 Å (Figure 4), corresponding to the mesopores, which is in close agreement with the isotherms (Figure 4).

Table 2 lists the textural characterization of the activated carbon, and a mesoporous structure can be verified. This characteristic is attributed to the activation method using phosphoric acid since this

activating agent contributes to increase the surface area of the adsorbents (Brito et al., 2017; da Silva Lacerda et al., 2015; Lim et al., 2010; Reffas et al., 2010).

Table 2. Textural properties of activated carbon produced from defective coffee beans.

Sample	Specific surface area ($\text{m}^2 \text{g}^{-1}$)	Pore diameter (nm) ^a	Mesopore volume ($\text{cm}^3 \text{g}^{-1}$)	Micropore volume ($\text{cm}^3 \text{g}^{-1}$)
AC from DCB	314.0131	4.8574	0.2035	0.0308

^a Maximum pore size distribution.

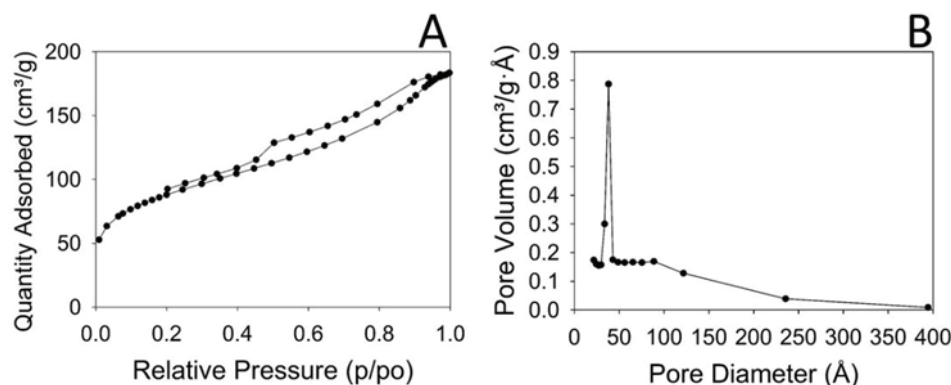


Figure 4. N_2 adsorption/desorption isotherm at 77 K for the activated carbon obtained from defective coffee beans (A) and pore volume distribution of AC from DCB (B).

Raman spectra

Figure 5 shows the Raman spectrum of the AC sample from DCB, as well as the procedure performed for the exclusion of the baseline. By analyzing the shape of the Raman D and G bands, it is possible to evaluate the degree of crystallinity or amorphization of carbonaceous materials. In these materials, the D band corresponds to the mode induced by disorder, while the G band is related to the tangential stretching mode (Ferrari & Robertson, 2000; 2001; Ribeiro-Soares et al., 2013).

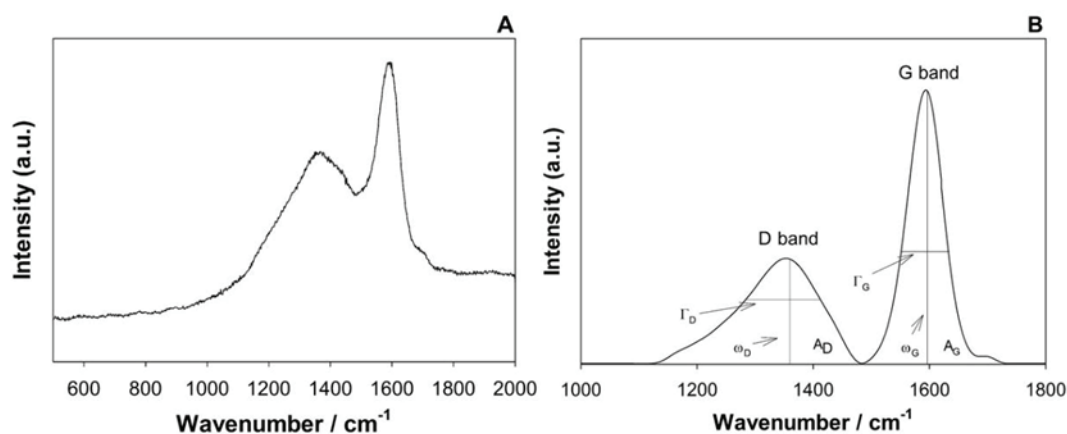


Figure 5. (A) Raman spectra of the activated carbons produced from defective coffee beans. (B) Procedure performed for baseline exclusion between 1100 cm^{-1} and 1700 cm^{-1} for all spectra of AC from DCB samples followed by a fitting procedure using Gauss-Lorentzian peaks. The parameters of interest were: integrated area of D (A_D) and G (A_G) peaks, D (ω_D) and G (ω_G) wavenumbers peaks, and D (Γ_D) and G (Γ_G) band full-width at half maximum. The spectrum was obtained using a laser at 532 nm.

An adjustment procedure was performed to exclude the baseline from 800 to 1900 cm^{-1} in all spectra analyzed (Figure 5 B) using the Raman Spectroscopy Software LabSpec v.5. Two peaks in Gauss-Lorentzian form were then adjusted to the spectra of the AC from DCB samples for acquisition of the integrated parameters D and G peaks (A_D and A_G), D (ω_D) and G (ω_G) wavenumbers bands, and D (Γ_D) and G (Γ_G) band full-width at half maximum, respectively.

Results of the D wavenumber band and full-width at half maximum were observed in the range of $1,349 \text{ cm}^{-1} < \omega_D < 1,353 \text{ cm}^{-1}$ and $155.64 \text{ cm}^{-1} < \Gamma_D < 160.45 \text{ cm}^{-1}$, while the G wavenumber band and G full-width at half maximum band ranged from $1,594 \text{ cm}^{-1} < \omega_G < 1,597 \text{ cm}^{-1}$ and $67.84 \text{ cm}^{-1} < \Gamma_G < 69.21 \text{ cm}^{-1}$. In general,

carbons from the AC sample from DCB exhibited Γ_G distribution similar to those found by other authors for biochar (Pagano et al., 2016; Ribeiro-Soares et al., 2013).

The crystallite size (L_a) is a concept used to estimate the relative degree of disorder in carbonaceous graphitic materials. The parameter used to estimate crystallinity is the G bandwidth (Cançado, Takai, & Enoki, 2006; Ribeiro-Soares et al., 2013). In this study L_a for activated carbons was estimated by a linear correlation (Equation 9), which applies to a wide range of carbon nanostructures (Cançado et al., 2006; Ribeiro-Soares et al., 2013):

$$L_a = \frac{496}{[\Gamma_G - 15]} \quad (9)$$

The L_a module predicted by Eq. (10) for the AC sample from DCB was approximately 9.31 ± 0.14 nm (Martins Ferreira et al., 2010; Pagano et al., 2016; Ribeiro-Soares et al., 2013), where this value is higher than that encountered for carbonaceous materials naturally found in anthropogenic soils, which present L_a in the range of 3 to 5 nm. However, for biomass coals obtained under conditions similar to those of this work, L_a results ranged from 9 to 12 nm, which is in good agreement with data reported in the literature (Martins Ferreira et al., 2010; Pagano et al., 2016; Ribeiro-Soares et al., 2013). This result suggests that the activated carbon presents high crystallinity and large amounts of inert and persistent degradation materials, making it unsuitable for application as a soil fertilizer (Ferrari & Robertson, 2000; Ribeiro-Soares et al., 2013). Nevertheless, the adsorptive capacity results of AC from DCB indicate the potential of this adsorbent for use in water and wastewater treatments for the removal of nutrients.

Determination of the point of zero charge and total ionic capacity

The point of zero charge is an important parameter since the pH affects the dissociation of active site groups on the adsorbent surface. The activated carbon produced from DCB presented acidic pH_{pzc} (2.0), which may be due to the formation of acid groups on the surface from phosphoric acid. The point of zero charge obtained in this experiment was lower than that obtained by Brito et al. (2017) for activated carbon from yellow mombin fruit stones ($\text{pH}_{\text{pzc}} = 5.2$).

Adsorption assays

Adsorption assays of whey proteins on the activated carbon produced from DCB were carried out at different pH values. From the results of the adsorption capacity, the highest value of q was obtained at pH 2.5 ($q = 239.1781 \pm 14.5924$ mg g^{-1}), suggesting that it is the ideal pH for further assays. The optimum pH was lower than the isoelectric point of whey protein (4.8 to 5.2), and at pH 2.5 the protein is positively charged. Therefore, the adsorption occurred due to cation exchange between the adsorbent surface and the protein (Schmitt, Sanchez, Desobry-Banon, & Hardy, 1998). This is in agreement with the point of zero charge found, which was close to pH 2.0. At pH above the point of zero charge, the adsorbent surface is more negatively charged and thus adsorbs cations from the solution (Vieira et al., 2010).

The adsorptive capacity was lower at pH 4.5 ($q = 144.5383 \pm 2.2806$ mg g^{-1}), possibly because this pH value is closest to the isoelectric point of whey protein (4.8 to 5.2), so protein-protein interactions are strong enough to cause protein aggregation instead of protein-activated carbon interactions. At pH 7.5 the adsorptive capacity was 188.4688 mg g^{-1} (± 5.5065 mg g^{-1}) and higher than at pH 4.5. Despite the electrostatic repulsion between the negatively charged whey protein and the activated carbons surface, which also had a negative charge, at pH 7.5 the adsorption process continues to occur probably due to the lower energy of electrostatic repulsion in comparison with the hydrophobic interaction (Wang, Zhou, Hong, & Zhang, 2012).

Pereira et al. (2014) tested activated carbon from yellow mombin seeds (*Spondias purpurea* L.) and cocoa shells (*Theobroma cacao* L.) using either phosphoric acid or ZnCl_2 as the activating agent and obtained maximum adsorption capacities at pH 7.0 for α -lactalbumin (193.54 mg g^{-1}) and BSA (188.29 mg g^{-1}). The adsorption capacities observed in the present study can be considered high and demonstrate the efficiency of the precursor material and the activation method.

Adsorption kinetics

The variation in the amount of whey protein adsorbed on the activated carbon, according to time, is graphically shown in Figure 6. The adsorption kinetic models were fitted to the experimental results, and the coefficients of determination obtained were greater than 0.93, as listed in Table 3, with the parameters of the three models adjusted.

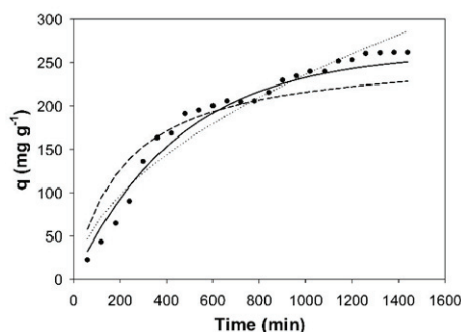


Figure 6. Experimental results (•) and adjusted models for adsorption kinetics of fresh whey protein on the activated carbon produced from defective coffee beans. Pseudo first-order model (—); Pseudo second-order model (---) and Intraparticle diffusion model (.....).

The pseudo first-order model best fit to the experimental data (Figure 6 and Table 3). The predicted adsorption capacity ($q_{t \text{ predicted}}$) for the time of 24h (263.2353 mg g^{-1}) and experimental ($q_{e \text{ experimental}} = 261.9576 \text{ mg g}^{-1}$) were similar, which also confirms that the pseudo first-order model was the most adequate to explain whey protein adsorption.

Table 3. Adjusted Parameters of the adsorption kinetics models.

Pseudo first-order					
$k_1 (\text{min.}^{-1})$		$q_t \text{ predicted} (\text{mg g}^{-1})$	$q_e \text{ experimental} (\text{mg g}^{-1})$	R^2	RMSE
0.0023		263.2353	261.9576	0.9969	11.2695
Pseudo second-order					
$k_2 (\text{g mg}^{-1} \text{min.}^{-1})$	$h (\text{mg g}^{-1} \text{min.}^{-1})$	$q_t \text{ predicted} (\text{mg g}^{-1})$	$q_e \text{ experimental} (\text{mg g}^{-1})$	R^2	RMSE
1.80×10^{-5}	1.2352	228.3299	261.9576	0.9816	27.7492
Intraparticle diffusion model					
k	$k_{\text{dif}} (\text{mg g}^{-1} \text{min.}^{-1/2})$	$q_t \text{ predicted} (\text{mg g}^{-1})$	$q_e \text{ experimental} (\text{mg g}^{-1})$	R^2	RMSE
-14.4977	7.9324	286.5157	261.9576	0.9359	17.7096

The amount of protein adsorbed during the first hours increased faster than over the remaining time. According to Li, Bruce and Hobday (1999), this behavior can be due to the presence of two chemically different adsorptive sites or due to different diffusion rates. The initial rate is higher because the adsorbate has easy access to the macropore active sites, and then it decreases due to slower diffusion within the mesopores and micropores of the activated carbon. This slower rate is maintained until the adsorption capacity remains constant, which occurred at 1,200 min. (20h).

Sarvi et al. (2014) examined the adsorption kinetics of dairy proteins on functionalized silica materials. The authors reported that at the beginning of the adsorption process, proteins preferably adsorb on the external surfaces and at a relatively high rate, and then in a second stage intraparticle diffusions become significant because the proteins have to penetrate the interior of the material to access the internal active sites.

Adsorption isotherms

The adsorption isotherms were determined for fresh whey protein on the activated carbon at 25°C (Figure 7), and Table 4 lists the adjusted parameters of the Langmuir and Freundlich models.

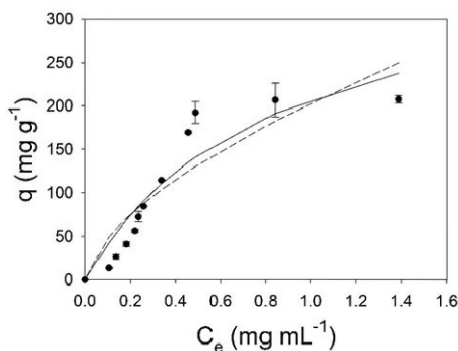


Figure 7. Experimental results (•) and adjusted models for adsorption isotherms of fresh whey proteins on the DCB activated carbon at pH 2.5 and 25°C, for 24 h. A 0.01 g mass of dried activated carbon was incubated with 10 mL of protein solution and maintained under 50 rpm agitation. Langmuir isotherm (—) and Freundlich isotherm (---).

Table 4. Langmuir and Freundlich parameters for the adsorption of fresh whey protein on the activated carbon produced from defective coffee beans.

Model parameters	q_{\max} (mg g ⁻¹)	Pr	K_d (mg mL ⁻¹)	Pr	R ²	RMSE
Langmuir	378.4380	0.0022	0.8177	0.0410	0.88	25.09
	K_f (mL mg ⁻¹)	Pr	n	Pr	R ²	RMSE
Freundlich	203.9864	0.0001	0.6234	0.0003	0.80	31.88

The models fit well to the experimental data for the concentration studied, presenting high values for the coefficient of determination (R²). The Langmuir model showed the best adjustment. For this model, the maximum adsorption capacity was 378.4380 mg of fresh whey protein per gram of activated carbon, which is comparable to results found with other adsorbents (Andrade et al., 2018; Fontan et al., 2013; Machado et al., 2015; Pereira et al., 2014). Sarvi et al. (2014) studied the adsorption of dairy protein and found q values of 310 mg of α -lactalbumin g⁻¹ on functionalized silica adsorbent and 173 mg of β -lactoglobulin g⁻¹ on the same adsorbent. Pereira et al. (2014) obtained q values for α -lactalbumin and BSA of 213.11 mg g⁻¹ and 58.266 mg g⁻¹ on activated carbon from cocoa shells and yellow mombin seeds, respectively. These authors found better adsorption for α -lactalbumin due to the smaller size of this protein, favoring greater interaction with the active sites of the adsorbent.

Conclusion

The DCB demonstrated to be a promising precursor material for activated carbon. The produced AC was characterized as a mesoporous material. Activated carbon presented crystallinity structure. A pH of 2.5 is the most suitable for the whey protein adsorptive process and the pH_{pzc} was close to pH 2.0, suggesting that adsorption occurred due to electrostatic interactions between the protein and adsorbent surface, which is negatively charged. The pseudo first-order model was most adequate to explain the adsorptive mechanism of whey protein using the AC obtained from defective coffee beans. Regarding equilibrium data, Langmuir model adjusted satisfactorily to the experimental results.

Acknowledgements

The authors thank the Center of Analysis and Chemical Prospecting of the Federal University of Lavras, CAPES, FAPEMIG (Grants N°. TEC - APQ-00647-17, CEX-APQ-01865-17, N°. TEC-AUC-00026-16, N°. RED-00185-16, N°. RED-00282-16), CNPq (Grant No. 310813/2017-4), and FINEP (02/2014 NANO N°. 0501/16, and the 02/2016 project) for the financial and equipment support. J.R-S. acknowledges support from the Pró-Reitoria de Pesquisa (UFLA) and the prize L'ORÉAL-UNESCO- For Women in Science Prize - Brazil/2017.

References

- Abd El-Salam, M. H., & El-Shibiny, S. (2017). Chapter 12 - Separation of bioactive whey proteins and peptides A2 - Grumezescu, Alexandru Mihai. In A. M. Holban (Ed.), *Ingredients extraction by physicochemical methods in food* (p. 463-494): Oxford, UK: Academic Press. DOI: 10.1016/B978-0-12-811521-3.00012-0
- Andrade, S. N., Veloso, C. M., Fontan, R. C. I., Bonomo, R. C. F., Santos, L. S., Brito, M. J. P., & Diniz, G. A. (2018). Chemical-activated carbon from coconut (*Cocos nucifera*) endocarp waste and its application in the adsorption of β -lactoglobulin protein. *Revista Mexicana de Ingeniería Química*, 17(2), 463-475. DOI: 10.24275/10.24275/uam/izt/dcbi/revmexingquim/2018v17n2/Andrade
- AOAC. (2012). *Official Methods of Analysis of AOAC International* (19th ed.). Gaithersburg, US: AOAC International.
- Arvind, D., & Hegde, G. (2015). Activated carbon nanospheres derived from bio-waste materials for supercapacitor applications – a review. *RSC Advances*, 5(107), 88339-88352. DOI: 10.1039/C5RA19392C
- Baldasso, C., Barros, T. C., & Tessaro, I. C. (2011). Concentration and purification of whey proteins by ultrafiltration. *Desalination*, 278(1), 381-386. DOI: 10.1016/j.desal.2011.05.055
- Bhatnagar, A., Sillanpää, M., & Witek-Krowiak, A. (2015). Agricultural waste peels as versatile biomass for water purification – A review. *Chemical Engineering Journal*, 270(Supplement C), 244-271. DOI: 10.1016/j.cej.2015.01.135

- Bogahawaththa, D., Chandrapala, J., & Vasiljevic, T. (2017). Thermal denaturation of bovine immunoglobulin G and its association with other whey proteins. *Food Hydrocolloids*, 72(Supplement C), 350-357. DOI: 10.1016/j.foodhyd.2017.06.017
- Bradford, M. M. (1976). A rapid and sensitive method for the quantitation of microgram quantities of protein utilizing the principle of protein-dye binding. *Analytical Biochemistry*, 72(1), 248-254. DOI: 10.1016/0003-2697(76)90527-3
- Brito, M. J. P., Veloso, C. M., Bonomo, R. C. F., Fontan, R. d. C. I., Santos, L. S., & Monteiro, K. A. (2017). Activated carbons preparation from yellow mombin fruit stones for lipase immobilization. *Fuel Processing Technology*, 156, 421-428. DOI: 10.1016/j.fuproc.2016.10.003
- Cançado, L. G., Takai, K., & Enoki, T. (2006). General equation for the determination of the crystallite size L_a of nanographite by Raman spectroscopy. *Applied Physics Letters*, 88(16), 163106. DOI: 10.1063/1.2196057
- Corbatón-Báguena, M. J., Álvarez-Blanco, S., & Vincent-Vela, M.-C. (2018). Evaluation of fouling resistances during the ultrafiltration of whey model solutions. *Journal of Cleaner Production*, 172(Supplement C), 358-367. DOI: 10.1016/j.jclepro.2017.10.149
- Da Silva Lacerda, V., López-Sotelo, J. B., Correa-Guimarães, A., Hernández-Navarro, S., Sánchez-Báscones, M., Navas-Gracia, L. M., ... Martín-Gil, J. (2015). Rhodamine B removal with activated carbons obtained from lignocellulosic waste. *Journal of Environmental Management*, 155, 67-76. DOI: 10.1016/j.jenvman.2015.03.007
- Damar Huner, I., & Gulec, H. A. (2017). Fouling behavior of poly(ether)sulfone ultrafiltration membrane during concentration of whey proteins: Effect of hydrophilic modification using atmospheric pressure argon jet plasma. *Colloids and Surfaces B: Biointerfaces*, 160(Supplement C), 510-519. DOI: 10.1016/j.colsurfb.2017.10.003
- Eugenia Lucena, M., Alvarez, S., Menéndez, C., Riera, F. A., & Alvarez, R. (2007). α -Lactalbumin precipitation from commercial whey protein concentrates. *Separation and Purification Technology*, 52(3), 446-453. DOI: 10.1016/j.seppur.2006.05.024
- Ferrari, A. C., & Robertson, J. (2000). Interpretation of Raman spectra of disordered and amorphous carbon. *Physical Review B*, 61(20), 14095-14107. DOI: 10.1103/PhysRevB.61.14095
- Ferrari, A. C., & Robertson, J. (2001). Resonant Raman spectroscopy of disordered, amorphous, and diamondlike carbon. *Physical Review B*, 64(7), 075414. DOI: 10.1103/PhysRevB.64.075414
- Fontan, R. C. I., Minim, L. A., Bonomo, R. C. F., da Silva, L. H. M., & Minim, V. P. R. (2013). Adsorption isotherms and thermodynamics of α -lactalbumin on an anionic exchanger. *Fluid Phase Equilibria*, 348(Supplement C), 39-44. DOI: 10.1016/j.fluid.2013.03.027
- Fritzen-Freire, C. B., Prudêncio, E. S., Amboni, R. D. M. C., Pinto, S. S., Negrão-Murakami, A. N., & Murakami, F. S. (2012). Microencapsulation of bifidobacteria by spray drying in the presence of prebiotics. *Food Research International*, 45(1), 306-312. DOI: 10.1016/j.foodres.2011.09.020
- Ganju, S., & Gogate, P. R. (2017). A review on approaches for efficient recovery of whey proteins from dairy industry effluents. *Journal of Food Engineering*, 215, 84-96. DOI: 10.1016/j.jfoodeng.2017.07.021
- Gonçalves, M., Guerreiro, M. C., Oliveira, L. C. A., Solar, C., Nazarro, M., & Sapag, K. (2013). Micro mesoporous activated carbon from coffee husk as biomass waste for environmental applications. *Waste and Biomass Valorization*, 4(2), 395-400. DOI: 10.1007/s12649-012-9163-1
- Hirata, M., Kawasaki, N., Nakamura, T., Matsumoto, K., Kabayama, M., Tamura, T., & Tanada, S. (2002). Adsorption of dyes onto carbonaceous materials produced from coffee grounds by microwave treatment. *Journal of Colloid and Interface Science*, 254(1), 17-22. DOI: 10.1006/jcis.2002.8570
- Ho, Y. S., & McKay, G. (1998). Sorption of dye from aqueous solution by peat. *Chemical Engineering Journal*, 70(2), 115-124. DOI: 10.1016/S0923-0467(98)00076-1
- Hosseini, S. F., Zandi, M., Rezaei, M., & Farahmandghavi, F. (2013). Two-step method for encapsulation of oregano essential oil in chitosan nanoparticles: Preparation, characterization and in vitro release study. *Carbohydrate Polymers*, 95(1), 50-56. DOI: 10.1016/j.carbpol.2013.02.031
- International Union of Pure and Applied Chemistry [IUPAC]. (1985). Reporting physisorption data for gas solid systems with special reference to the determination of surface area and porosity. *Pure & Applied Chemistry*, 57(4), 603-619. DOI: 10.1351/pac198557040603

- Jain, A., & Tripathi, S. K. (2014). Fabrication and characterization of energy storing supercapacitor devices using coconut shell based activated charcoal electrode. *Materials Science and Engineering B*, 183, 54-60. DOI: 10.1016/j.mseb.2013.12.004
- Li, P. H. Y., Bruce, R. L., & Hobday, M. D. (1999). A pseudo first order rate model for the adsorption of an organic adsorbate in aqueous solution. *Journal of Chemical Technology & Biotechnology*, 74(1), 55-59. DOI: 10.1002/(SICI)1097-4660(199901)74:1<55::AID-JCTB984>3.0.CO;2-D
- Lim, W. C., Srinivasakannan, C., & Balasubramanian, N. (2010). Activation of palm shells by phosphoric acid impregnation for high yielding activated carbon. *Journal of Analytical and Applied Pyrolysis*, 88(2), 181-186. DOI: 10.1016/j.jaap.2010.04.004
- Liou, T.-H. (2010). Development of mesoporous structure and high adsorption capacity of biomass-based activated carbon by phosphoric acid and zinc chloride activation. *Chemical Engineering Journal*, 158(2), 129-142. DOI: 10.1016/j.cej.2009.12.016
- Machado, A. P. d. F., Minim, L. A., Fontan, R. d. C. I., Minim, V. P. R., Gonçalves, G. R. F., & Mól, P. C. G. (2015). Adsorptive behavior of α -lactalbumin on cation-exchange supermacroporous monolithic column. *Fluid Phase Equilibria*, 401(Supplement C), 64-69. DOI: 10.1016/j.fluid.2015.05.021
- Martins Ferreira, E. H., Moutinho, M. V. O., Stavale, F., Lucchese, M. M., Capaz, R. B., Achete, C. A., & Jorio, A. (2010). Evolution of the Raman spectra from single-, few-, and many-layer graphene with increasing disorder. *Physical Review B*, 82(12), 125429. DOI: 10.1103/PhysRevB.82.125429
- Pagano, M. C., Ribeiro-Soares, J., Cançado, L. G., Falcão, N. P. S., Gonçalves, V. N., Rosa, L. H., ..., Jorio, A. (2016). Depth dependence of black carbon structure, elemental and microbiological composition in anthropic Amazonian dark soil. *Soil and Tillage Research*, 155, 298-307. DOI: 10.1016/j.still.2015.09.001
- Pereira, R. G., Veloso, C. M., da Silva, N. M., de Sousa, L. F., Bonomo, R. C. F., de Souza, A. O., ... Fontan, R. d. C. I. (2014). Preparation of activated carbons from cocoa shells and siriguela seeds using H_3PO_4 and $ZnCl_2$ as activating agents for BSA and α -lactalbumin adsorption. *Fuel Processing Technology*, 126, 476-486. DOI: 10.1016/j.fuproc.2014.06.001
- Prazeres, A. R., Carvalho, F., & Rivas, J. (2012). Cheese whey management: A review. *Journal of Environmental Management*, 110(Supplement C), 48-68. DOI: 10.1016/j.jenvman.2012.05.018
- Ramos, P. H., Guerreiro, M. C., Resende, E. C., & Gonçalves, M. (2009). Produção e caracterização de carvão ativado produzido a partir do defeito preto, verde, ardido (PVA) do café. *Química Nova*, 329(5), 1139-1143. DOI: 10.1590/S0100-40422009000500011
- Reffas, A., Bernardet, V., David, B., Reinert, L., Lehocine, M. B., Dubois, M., ... Duclaux, L. (2010). Carbons prepared from coffee grounds by H_3PO_4 activation: Characterization and adsorption of methylene blue and Nylosan Red N-2RBL. *Journal of Hazardous Materials*, 175(1), 779-788. DOI: 10.1016/j.jhazmat.2009.10.076
- Ribeiro-Soares, J., Cançado, L. G., Falcão, N. P. S., Martins Ferreira, E. H., Achete, C. A., & Jorio, A. (2013). The use of Raman spectroscopy to characterize the carbon materials found in Amazonian anthrosoils. *Journal of Raman Spectroscopy*, 44(2), 283-289. DOI: 10.1002/jrs.4191
- Roy, S., Das, P., & Sengupta, S. (2017). Treatability study using novel activated carbon prepared from rice husk: Column study, optimization using response surface methodology and mathematical modeling. *Process Safety and Environmental Protection*, 105, 184-193. DOI: 10.1016/j.psep.2016.11.007
- Santana, G. M., Lelis, R. C. C., Jaguaribe, E. F., Morais, R., M., Paes, J. B., & Trugilho, P. F. (2017). Development of activated carbon from bamboo (*Bambusa vulgaris*) for pesticide removal from aqueous solutions. *Cerne*, 23(1), 123-132. DOI: 10.1590/01047760201723012256
- Sarvi, M. N., Budianto Bee, T., Gooi, C. K., Woonton, B. W., Gee, M. L., & O'Connor, A. J. (2014). Development of functionalized mesoporous silica for adsorption and separation of dairy proteins. *Chemical Engineering Journal*, 235(Supplement C), 244-251. DOI: 10.1016/j.cej.2013.09.036
- Schmitt, C., Sanchez, C., Desobry-Banon, S., & Hardy, J. (1998). Structure and technofunctional properties of protein-polysaccharide complexes: a review. *Critical Reviews in Food Science and Nutrition*, 38(8), 689-753. DOI: 10.1080/10408699891274354
- Vieira, A. P., Santana, S. A. A., Bezerra, C. W. B., Silva, H. A. S., Melo, J. C. P., Silva Filho, E. C., & Airoidi, C. (2010). Copper sorption from aqueous solutions and sugar cane spirits by chemically modified babassu

coconut (*Orbignya speciosa*) mesocarp. *Chemical Engineering Journal*, 161(1), 99-105. DOI: 10.1016/j.cej.2010.04.036

Wang, K., Zhou, C., Hong, Y., & Zhang, X. (2012). A review of protein adsorption on bioceramics. *Interface Focus*, 2(3), 259-277. DOI: 10.1098/rsfs.2012.0012

Yang, J., & Qiu, K. (2011). Development of high surface area mesoporous activated carbons from herb residues. *Chemical Engineering Journal*, 167(1), 148-154. DOI: 10.1016/j.cej.2010.12.013